

# PROCEEDINGS OF SPIE

[SPIDigitalLibrary.org/conference-proceedings-of-spie](https://spiedigitallibrary.org/conference-proceedings-of-spie)

## Characterization and imaging of nanostructured materials using tabletop extreme ultraviolet light sources

Robert Karl, Joshua Knobloch, Travis Frazer, Michael Tanksalvala, Christina Porter, et al.

Robert Karl, Joshua Knobloch, Travis Frazer, Michael Tanksalvala, Christina Porter, Charles Bevis, Weilun Chao, Begoña Abad Mayor, Daniel Adams, Giulia F. Mancini, Jorge N. Hernandez-Charpak, Henry Kapteyn, Margaret Murnane, "Characterization and imaging of nanostructured materials using tabletop extreme ultraviolet light sources," Proc. SPIE 10585, Metrology, Inspection, and Process Control for Microlithography XXXII, 105850N (13 March 2018); doi: 10.1117/12.2297223

**SPIE.**

Event: SPIE Advanced Lithography, 2018, San Jose, California, United States

# Characterization and imaging of nanostructured materials using tabletop extreme ultraviolet light sources

Robert Karl Jr.<sup>1,\*</sup>, Joshua Knobloch<sup>1</sup>, Travis Frazer<sup>1</sup>, Michael Tanksalvala<sup>1</sup>, Christina Porter<sup>1</sup>, Charles Bevis<sup>1</sup>, Weilun Chao<sup>2</sup>, Begoña Abad Mayor<sup>1</sup>, Daniel Adams<sup>1</sup>, Giulia Mancini<sup>1</sup>, Jorge N. Hernandez-Charpak<sup>1</sup>, Henry Kapteyn<sup>1</sup>, and Margaret Murnane<sup>1</sup>

<sup>1</sup>JILA, 440 UCB, University of Colorado, Boulder, CO 80309 USA

<sup>2</sup>Center for X-Ray Optics, Lawrence Berkeley National Laboratory, Berkeley, CA 94720

## ABSTRACT

Using a tabletop coherent extreme ultraviolet source, we extend current nanoscale metrology capabilities with applications spanning from new models of nanoscale transport and materials, to nanoscale device fabrication. We measure the ultrafast dynamics of acoustic waves in materials; by analyzing the material's response, we can extract elastic properties of films as thin as 11nm. We extend this capability to a spatially resolved imaging modality by using coherent diffractive imaging to image the acoustic waves in nanostructures as they propagate. This will allow for spatially resolved characterization of the elastic properties of non-isotropic materials.

**Keywords:** Ultrafast x-rays, nanometrology, ultrathin films, nano-mechanical properties, coherent diffractive imaging, ptychography, photoacoustic

## 1. INTRODUCTION

Modern nanofabrication techniques allow for creation of devices with characteristic length-scales as small as a few nm. However, many characterization techniques rely on optical techniques to characterize these films and structures, which becomes increasingly problematic at scale lengths small compared with optical wavelengths. To enable iterative design and process control of nanosystems, better functional metrology tools are needed. In this work, we use tabletop coherent extreme ultraviolet (EUV) light generated through high harmonic generation (HHG) in a pump probe experiment to probe and image nanoscale systems, extracting material properties on very small length-scales.

In this work we present results of two experiments aimed at understanding material properties at the nanoscale. In the first experiment, we use an ultrafast pump probe experiment to interrogate the acoustic dynamics of thin films in order to extract the Young's modulus and Poisson's ratio, thereby fully characterizing the elastic tensor of sub-100nm films. In the second experiment, we apply stroboscopic ptychography coherent diffractive imaging to spatially and temporally resolve the propagation of acoustic waves.

## 2. THIN FILM CHARACTERIZATION

We have previously utilized this photoacoustic EUV nanometrology to fully characterize the elastic tensor of isotropic 66-132nm low dielectric constant,  $k$ , ultrathin films with Young's modulus varying from 5GPa to 197GPa and average bond coordination varying from 2.1 to 3.2<sup>1</sup>. We measure a series of a-SiOC:H ultrathin films, where the properties are nominally constant while the thicknesses differ to look for possible deviations from the bulk properties.

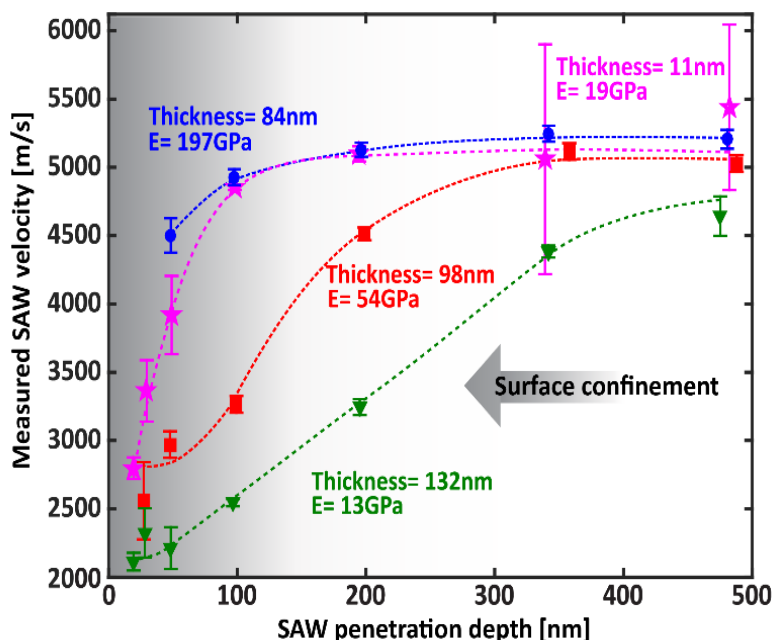


Figure 1 As the periodicity of the acoustic wave is varied, the confinement to the thin film changes<sup>1</sup>. By measuring the surface acoustic wave velocity for many penetration depths, we can measure the transition of substrate confinement to film confinement.

In similar fashion to the previous study<sup>1</sup>, we selectively probe different depths in the sample. This allows us to probe the elastic properties of the silicon substrate for large grating periodicities or those of the ultrathin film for very small grating periodicities, as well as measure the transition from one regime to the other. As seen in figure 1, the surface acoustic wave (SAW) velocities transition from that of silicon to that of the thin film at different penetration depths corresponding to different film thicknesses. By advancing our finite element methods used to account for the nanostructures' alteration of the acoustic velocities, we extract the full elastic tensor of the 10.9nm isotropic film, which represents the thinnest film fully characterized to date, even though the SAW was not completely confined to the film<sup>1</sup>.

### 3. STROBOSCOPIC ACOUSTIC IMAGING

In order to study the spatially dependent dynamics of these acoustic waves, we must probe our sample in a spatially resolved modality<sup>2</sup>. In our experiment shown in Fig. 1, the laser excitation pulse and the  $\lambda=30\text{nm}$  high harmonic probe illumination beam were both derived from a 23fs, 1.5mJ, 5kHz, Ti:Sapphire laser system (pre-commercial KMLabs DRAGON). Bright, phase-matched, spatially coherent HHG beams, with duration  $< 10$  fs, were produced by focusing most of the laser beam into a 5cm-long waveguide filled with 32 torr of argon gas. The residual laser light was rejected using a pair of super-polished silicon substrates set at Brewster's angle, together with a single 100nm Al filter. A single harmonic at a wavelength of 30nm (41eV) was then selected using a pair of multilayer mirrors set at 45 degrees. An ellipsoidal mirror at a  $5^\circ$  angle of incidence from the surface focused the HHG beam to a  $21\mu\text{m} \times 21\mu\text{m}$  diameter spot. The light diffracted from the sample was collected with an x-ray CCD, placed a distance of 36.5mm from the sample.

Our sample consisted of 20nm tall Ni nanostructures patterned on a Si wafer. To excite thermal and acoustic dynamics, we irradiated it with part of the 780 nm laser beam, at an incident fluence of  $7.7\text{mJ}/\text{cm}^2$  in a  $500\mu\text{m}$ -diameter spot. Snapshots of the sample were then collected at different time-delays (Fig. 1). Traditional methods of imaging are widely infeasible for EUV light, leading us to employ coherent diffractive imaging methods<sup>3,4</sup>, specifically ptychography<sup>5</sup>. In this modality, the probe beam is scanned over the sample so that each illuminated area overlaps with previously scanned areas, allowing for robust image recovery.

At each time delay, the sample was imaged using ptychographic CDI, which employs multiple diffraction patterns from overlapping fields of view. The transient response of the sample was retrieved from an analysis of the diffraction patterns from the Ni features at different time-delays between pump and probe pulses, which exhibit a sharp rise at zero

delay (time zero) due to  $<1$ ps thermal expansion, followed by oscillations due to longitudinal acoustic waves and surface acoustic waves launched within the Ni lines and Si substrate. The dynamic diffraction efficiency of the Ni lines was calculated following<sup>6</sup>, by computing the normalized difference in power in the 1st order diffraction peak and in the 0th order diffraction peak.

Figure 1c (yellow trace) plots the 1st order diffraction signal (where the rapid oscillations are due to longitudinal acoustic waves within the nanostructures, not random noise). To validate our measurement, we also extracted the signal from a single diffraction pattern from the ptychography scan (Fig.1c: blue triangles). The good agreement between the two data sets indicates that the acoustic dynamics we are imaging are consistent with those extracted spectroscopically, as expected for this uniform sample.

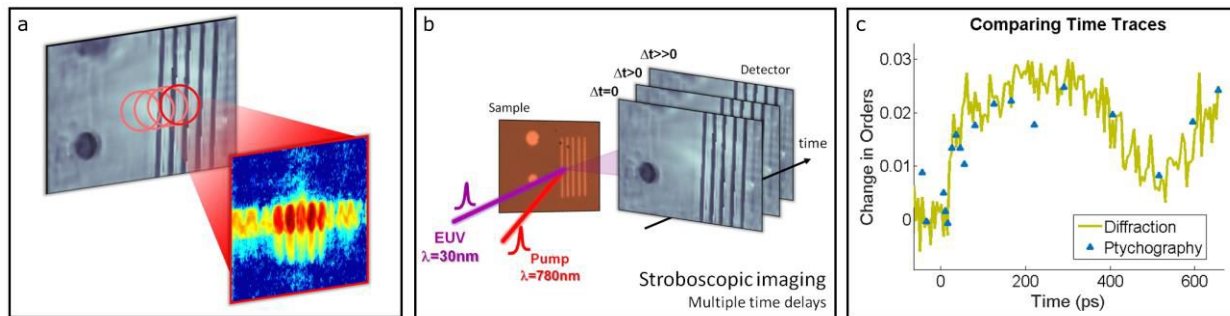


Figure 2. Experimental setup for full field EUV dynamic imaging on a tabletop. (a) A single image formed by ptychographic scanning CDI. (b) A series of stroboscopic images are reconstructed for every pump probe delay. (c) Plot of change in the 1st diffraction order power for a single diffraction pattern (yellow line) and for the diffraction patterns from the ptychographic data set (blue triangles), to validate the consistency of our data.

Ptychographic scans off a triangular nickel nanostructure were also taken at various pump probe delays. Images of a triangular nanostructure were reconstructed from these data sets using 10550 iterations of ePIE<sup>5</sup> with a MEP constraint<sup>7</sup> using a factor of 1 and 5 for the object and probe relaxation factors, respectively. 400 iterations of a position correction algorithm were used to refine the scan positions<sup>8</sup>. The end result is 30 complex images of the probe and the sample at various pump probe delays both with and without the pump illumination.

From the complex images, we can extract the dynamics of the nanostructure. This nanostructure is a Nickel isosceles triangle that is  $5\mu\text{m}$  wide,  $53\mu\text{m}$  long and  $20\text{nm}$  tall. In the first few picoseconds after the pump excitation, the structure undergoes thermal expansion and acoustic waves are launched in the nickel. After this, the waves propagate primarily along the short direction of the nanostructure as seen in figure 3.

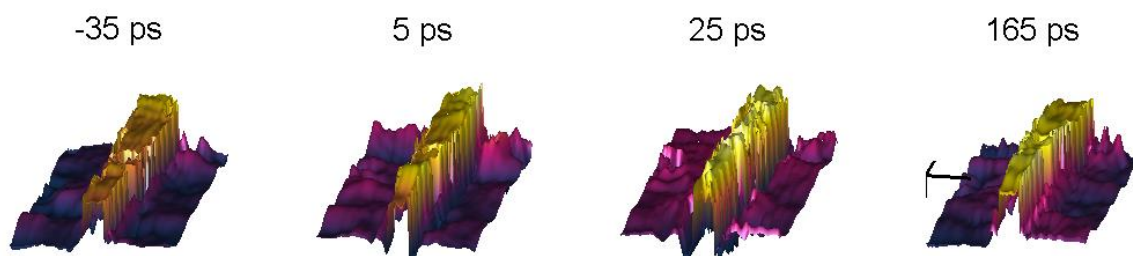


Figure 3: Ptychographic reconstructions of a nanostructure as a function of pump-probe delay. Spatially resolved propagation of acoustic waves in the nanostructure and the substrate are measured. The feature undergoes thermal expansion, which launches travelling surface acoustic waves in both the feature and the substrate. The scale bar is shared by all panels and is  $2\mu\text{m}$  in each transverse direction and  $0.5\text{nm}$  in the vertical.

## 4. CONCLUSIONS

We have demonstrated that using a coherent EUV source, we can characterize the elastic tensor of ultrathin films down to  $10.9\text{nm}$  thicknesses. This new understanding of ultrathin films demonstrates that coherent EUV beams present a new

nanometrology capability that can probe a wide range of novel complex materials. We further demonstrate the feasibility of extending this technique to a spatially resolved modality, allowing us to measure the propagation of acoustic waves in space and time. This will allow us to probe the elastic tensor of anisotropic materials, and let us understand the spatially varying elastic properties.

## 5. ACKNOWLEDGEMENTS

The authors acknowledge Marie Tripp and Sean W. King from Intel Corp. for lending their expertise in thin films, materials, and characterization. The authors would also like to thank their funding sources: NSF STC: DMR-1548924; DARPA PULSE: W31P4Q-13-1-0015, Gordon and Betty Moore Foundation's EPiQS Initiative through Grant GBMF: NSF MRSEC: DMR-1420620, an NDSEG fellowship, an NSF GRFP fellowship, a SRCEA fellowship program.

## 6. REFERENCES

- [1] Hernandez-Charpak, J. N., Hoogeboom-Pot, K. M., Li, Q., Frazer, T. D., Knobloch, J. L., Tripp, M., King, S. W., Anderson, E. H., Chao, W., Murnane, M. M., Kapteyn, H. C. and Nardi, D., "Full Characterization of the Mechanical Properties of 11-50 nm Ultrathin Films: Influence of Network Connectivity on the Poisson's Ratio," *Nano Lett.* **17**(4), 2178–2183 (2017).
- [2] Karl, R., Mancini, G., Gardner, D., Shanblatt, E., Knobloch, J., Frazer, T., Hernandez-Charpak, J. N., Mayor, B. A., Tanksalvala, M., Porter, C., Bevis, C., Adams, D., Kapteyn, H. and Murnane, M., "Full-field functional imaging of nanoscale dynamics using tabletop high harmonics," *Conf. Lasers Electro Opt. Postdeadline Part F43-C*, 0–1 (2017).
- [3] Fienup, J. R., "Phase retrieval algorithms: a comparison.," *Appl. Opt.* **21**(15), 2758–2769 (1982).
- [4] Chapman, H. N. and Nugent, K. A., "Coherent lensless X-ray imaging," *Nat. Photonics* **4**(12), 833–839 (2010).
- [5] Maiden, A. M. and Rodenburg, J. M., "An improved ptychographical phase retrieval algorithm for diffractive imaging.," *Ultramicroscopy* **109**(10), 1256–1262 (2009).
- [6] Hoogeboom-Pot, K., Hernandez-Charpak, J. N., Anderson, E., Gu, X., Yang, R., Kapteyn, H., Murnane, M. and Nardi, D., "A new regime of nanoscale thermal transport: Collective diffusion counteracts dissipation inefficiency," *Proc. Natl. Acad. Sci.* **162**(16), 341–344 (2015).
- [7] Gardner, D. F., Tanksalvala, M., Shanblatt, E. R., Zhang, X., Galloway, B. R., Porter, C. L., Jr, R. K., Bevis, C., Adams, D. E., Kapteyn, H. C., Murnane, M. M. and Mancini, G. F., "Subwavelength coherent imaging of periodic samples using a 13.5 nm tabletop high-harmonic light source," *Nat. Photonics*(March), 1–6 (2017).
- [8] Zhang, F., Peterson, I., Vila-Comamala, J., Diaz, A., Berenguer, F., Bean, R., Chen, B., Menzel, A., Robinson, I. K. and Rodenburg, J. M., "Translation position determination in ptychographic coherent diffraction imaging.," *Opt. Express* **21**(11), 13592–13606 (2013).